

UAV Collision Avoidance Considering No-Fly-Zones^{*}

Hae-In Lee,^{*} Hyo-Sang Shin^{*} Antonios Tsourdos^{*}

^{*} School of Aerospace, Transport and Manufacturing, Cranfield
University, College Road, Cranfield, Bedfordshire, MK43 0AL, UK
(e-mail: haein.lee ; h.shin ; a.tsourdos@cranfield.ac.uk).

Abstract: This paper proposes a collision avoidance algorithm that ensures minimum separation between the vehicles considering multiple no-fly-zones. The proposed algorithm aims to provide a practical and efficient tactical de-confliction solution for Unmanned Aerial Vehicles (UAVs). The main idea is to utilise the differential geometry concept that computes the minimum heading angle change to avoid the obstacles, and to expand its applicability to polygonal obstacles. This paper validates the minimum separation and efficiency of the proposed algorithm both analytically and numerically.

Keywords: Collision Avoidance, Obstacle Avoidance, Unmanned Aerial Vehicle (UAV), Differential Geometry

1. INTRODUCTION

In accordance with the increasing interest on the versatile applicability of Unmanned Aerial Vehicles (UAVs), development of Unmanned aircraft Traffic Management (UTM) framework is becoming paramount. There are numerous researches, for instance U-Space in Europe, actively undergoing to develop a UTM solution that enables the end users to operate their UAVs with sufficient efficiency and safety. Even though UTM shares some similar services with manned Air Traffic Management (ATM), which is relatively well-established through the past decades, UTM has its distinctive characteristics in the key services such as strategic and tactical de-confliction. The algorithms developed for ATM may not guarantee safety and efficiency for UTM, due to their discrepancy in its scale, platform, and non-segregated operational airspace.

One of the most important services to be further developed and validated for UTM is collision avoidance algorithm, which guides each UAV to ensure safety distance between vehicles and no-fly-zones in in-flight stage. There have been several approaches proposed for UAV collision avoidance: rule-based approaches (Hwang et al., 2007; Hwang and Tomlin, 2002), geometry-based approaches, artificial potential field algorithms (Kelly III and Eby, 2000; Nieuwenhuisen et al., 2013; Sun et al., 2017), and numerical optimisation methods (Richards and How, 2002; Roberge et al., 2012; Yang et al., 2019). Rule-based approaches are easy to implement, but it requires to set different rules depending on the platforms and scenarios. Artificial potential field methods are also easy to implement, but it may suffer from so-called narrow channel problem. This occurs when the obstacles are dense so that the minimum separation is not guaranteed near the local

minima. Numerical optimisation methods can guarantee the minimum separation as well as optimising the energy or time, while the computational load is higher than the rule-based or artificial potential field methods.

The aforementioned collision avoidance methods have their own advantages and characteristics, but most of them are developed under the assumption that the obstacles have circular or elliptical shape (Yan et al., 2018). This assumption may not be practical nor efficient considering that no-fly-zones are usually large in scale and declared as 4D polygons. Approximating a large zone as cylindrical shape can lead to unnecessary deviation from the original flight plan, raising the risk on battery level. In urban environments, there could be even no feasible path inside the dense buildings that are approximated as cylindrical shape. Hence, consideration of irregular-shape obstacles into tactical de-confliction is a key element of a UTM solution expanding the operational boundary to challenging environments.

This paper proposes a geometry-based collision avoidance algorithm which can consider this practical issue: multiple irregular-shape obstacles. The proposed algorithm guarantees the minimum separation not only with moving intruders, but also with polygonal no-fly-zones or buildings. The differential geometry concept (Seo et al., 2013; Shin et al., 2008; White et al., 2011) is utilised to analytically guarantee the minimum separation with low computational cost. The key idea of the algorithm is to detect the line-of-sights with potential conflict, and to change the heading angle to avoid the conflict. Various performance measures – minimum separation, flight time to reach the waypoint, and computational cost – are compared with other collision avoidance methods to verify the safety, efficiency, and scalability of the algorithm, respectively.

The rest of the paper is composed as follows: problem formulation and some definitions are given in section 2.

^{*} This research was supported by EuroDRONE project (No. SJU/LC/0342-CRT) under European Union's Horizon 2020 research and innovation programme.

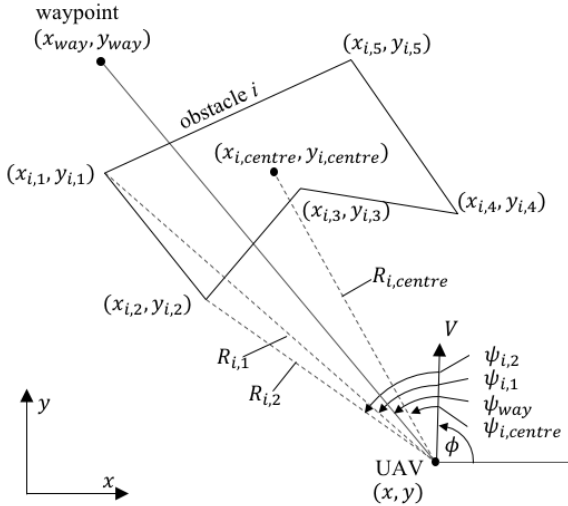


Fig. 1. Relative geometry of a UAV to a polygonal obstacle

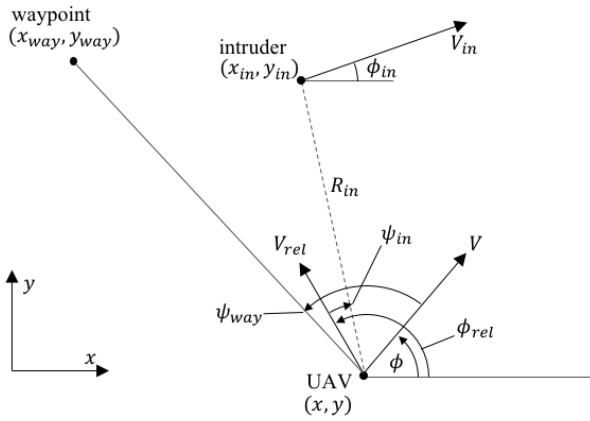


Fig. 2. Relative geometry of a UAV to an intruder

In section 3, the proposed collision avoidance algorithm and its theoretic analysis is addressed. The numerical simulations in section 4 validate and verify the proposed algorithm. Conclusions are given in section 5.

2. PROBLEM FORMULATION

Consider a 2D scenario with a UAV guided to a waypoint, and there exist multiple polygonal obstacles and an intruder. Then, the relative geometry of the UAV to the i -th polygonal obstacle is shown in Fig. 1. It is assumed that the polygonal obstacles include no-fly-zones, buildings and other obstacles that are fixed for a given time span, and the position of their feature points, $(x_{i,j}, y_{i,j})$, is known. The range ($R_{i,j}$'s) and bearing ($\psi_{i,j}$'s) of the i -th obstacle feature points are computed with respect to the position and velocity of the UAV, respectively. The range ($R_{i,centre}$) and bearing ($\psi_{i,centre}$) of the i -th obstacle's centre are defined to distinguish the feature points from other obstacles.

The relative geometry of the UAV to the intruder vehicle is shown in Fig. 2. It is assumed that the position (x_{in}, y_{in}) and velocity (V_{in}, ϕ_{in}) of the intruder are known within a certain range, either because the intruder is cooperative

or because its position and velocity are estimated through sensors. The range (R_{in}) and bearing (ψ_{in}) of the intruder are computed with respect to the position and relative velocity of the UAV. The ground speed of both the vehicle and intruder is assumed to be constant as V and V_{in} , respectively.

Based on the relative geometry of the UAV, the recognition and collision is defined as in (Seo et al., 2013):

Definition 1. (Recognition). The UAV is able to recognise

- the polygonal obstacle i if $R_i < R_{RC,i}$;
- the intruder if $R_{in} < R_{RC}$,

where $R_{RC,i}$ and R_{RC} are the recognition range of the i -th obstacle and the intruder, respectively.

Definition 2. (Collision). The UAV is collided with

- the polygonal obstacle i if $R_i < R_0$;
- the intruder if $R_{in} < R_0$,

where R_0 is the minimum separation.

3. COLLISION AVOIDANCE ALGORITHM

3.1 Conflict Detection Method

Any conflicting obstacles or intruders, which are in danger of collision, are detected. For each recognised polygonal obstacle i , two nodes that are most endangered of collision can be identified from:

$$j_L = \arg \max_j W \left(\psi_{i,j} + \sin^{-1} \frac{R_0}{R_{i,j}} - \psi_{i,centre} \right), \quad (1)$$

$$j_R = \arg \min_j W \left(\psi_{i,j} - \sin^{-1} \frac{R_0}{R_{i,j}} - \psi_{i,centre} \right),$$

where $W(\cdot)$ wraps the angle to $[-\pi, \pi]$, and the subscripts L and R stand for left and right-hand-side with respect to the line-of-sight to the obstacle's centre.

The bearing angle of the two nodes to ensure the minimum separation is:

$$\psi_{i,L} = W \left(\psi_{i,j_L} + \sin^{-1} \frac{R_0}{R_{i,j_L}} \right), \quad (2)$$

$$\psi_{i,R} = W \left(\psi_{i,j_R} - \sin^{-1} \frac{R_0}{R_{i,j_R}} \right).$$

Similarly for the recognised intruder, the bearing angle ensuring the minimum separation is obtained as:

$$\psi_{in,L} = W \left(\psi_{in} + \sin^{-1} \frac{R_0}{R_{in}} \right), \quad (3)$$

$$\psi_{in,R} = W \left(\psi_{in} - \sin^{-1} \frac{R_0}{R_{in}} \right).$$

Then, the union of the intervals can be obtained as:

$$\mathcal{I} = \left(\bigcup_i [\psi_{i,R}, \psi_{i,L}] \right) \cup [\psi_{in,R}, \psi_{in,L}]. \quad (4)$$

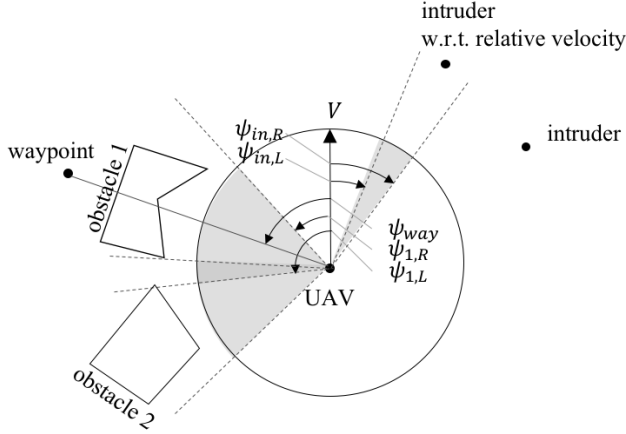


Fig. 3. Conflict Detection and Resolution Intervals

This set of intervals shows which line-of-sight leads to potential collision. Since the desired line-of-sight heads to the waypoint, the conflict is detected if:

$$\psi_{way} \in \mathcal{I}. \quad (5)$$

3.2 Conflict Resolution Method

If the conflict is detected, let us define the largest interval $[\psi_R, \psi_L] \subset \mathcal{I}$ which contains ψ_{way} . The conflict can be resolved by steering the UAV's heading angle either by ψ_R or ψ_L .

Note that this interval is different from the union of the intervals that contain ψ_{way} , i.e.,

$$\mathcal{I}' = \left(\bigcup_i \{[\psi_{i,R}, \psi_{i,L}] | \psi_{way} \in [\psi_{i,R}, \psi_{i,L}]\} \right) \cup \{[\psi_{in,R}, \psi_{in,L}] | \psi_{way} \in [\psi_{in,R}, \psi_{in,L}]\}, \quad (6)$$

which has been commonly used in previous works on differential geometry based collision avoidance (Seo et al., 2013; Shin et al., 2008). The physical meaning of computing \mathcal{I} and deriving the interval $[\psi_R, \psi_L]$ is to include the obstacle/intruder which does not directly intervene the UAV's line-of-sight to the waypoint, but overlaps with another one in direct conflict. This reduces the UAV's detour from the waypoint by foreseeing the potential conflicts, and resolves the chattering problem mentioned in the previous works. For instance, the set of intervals \mathcal{I} is visualised as grey area in Fig. 3. The largest interval in \mathcal{I} containing the waypoint is $[\psi_{2,L}, \psi_{1,R}]$, whereas the interval obtained from \mathcal{I}' is $[\psi_{1,L}, \psi_{1,R}]$. Steering of the UAV towards $\psi_{1,L}$ may result in unnecessary detour or chattering issue.

Once the interval $[\psi_R, \psi_L]$ is obtained from \mathcal{I} , the desired heading angle change is determined to minimise the detour from the waypoint as:

$$\psi_d = \begin{cases} \psi_R, & \text{if } |\psi_R - \psi_{way}| < |\psi_L - \psi_{way}|; \\ \psi_L, & \text{otherwise.} \end{cases} \quad (7)$$

Note that this choice of the heading angle change is to minimise the time to reach the waypoint. Otherwise to reduce control efforts, one may consider choosing the heading angle as:

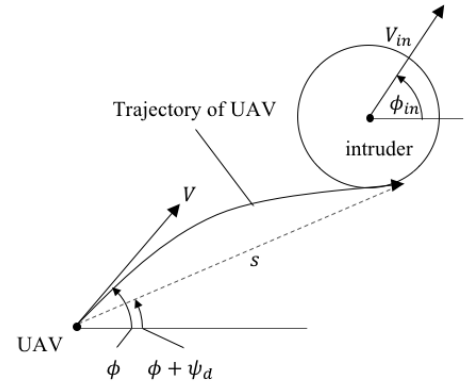


Fig. 4. Collision avoidance geometry of a UAV to an intruder

$$\psi_d = \begin{cases} \psi_R, & \text{if } |\psi_R| < |\psi_L|; \\ \psi_L, & \text{otherwise.} \end{cases} \quad (8)$$

The heading angle control to achieve the desired change ψ_d is suggested as:

$$\dot{\phi} = \frac{V_d}{\sqrt{R_d^2 - R_0^2}} \text{sgn} \psi_d + K \psi_d, \quad (9)$$

where V_d and R_d are relative velocity and range of the obstacle/intruder at the line-of-sight of ψ_d , respectively, and $K > 0$ is the control gain of the heading angle.

3.3 Minimum Separation Analysis

If the desired heading angle change ψ_d is properly computed, it has been proven that the minimum separation is guaranteed through the suggested heading angle control (Seo et al., 2013; Shin et al., 2008). Its characteristics and proof are briefly addressed in the following theorems:

Theorem 1. If the ground speed of the ownship UAV is greater than or equal to that of the intruder UAV, i.e. $V \geq V_{in}$, the proposed collision avoidance guarantees the minimum separation.

Proof. Let us define the Lyapunov function as:

$$V(\psi_d) = \frac{1}{2} \psi_d^2. \quad (10)$$

The derivative of the Lyapunov function is computed as:

$$\begin{aligned} \dot{V}(\psi_d) &= \psi_d \left(\dot{\phi}_{rel} - \left(\frac{V_d}{\sqrt{R_d^2 - R_0^2}} \text{sgn} \psi_d + K \psi_d \right) \right) \\ &= -K \psi_d^2 - \left(\frac{V_d}{\sqrt{R_d^2 - R_0^2}} \text{sgn} \psi_d - \dot{\phi}_{rel} \right) \psi_d, \end{aligned} \quad (11)$$

Assuming that the obstacles are assumed to be fixed and the intruder to be non-maneuvring, $\text{sgn} \dot{\phi}_{rel} = \text{sgn} \psi_d$. Also, the assumption on $V \geq V_{in}$ gives $|\dot{\phi}_{rel}| \leq V_d / \sqrt{R_d^2 - R_0^2}$ for all fixed obstacles and moving intruder. Hence, the Lyapunov function satisfies:

$$\dot{V}(\psi_d) \leq -K \psi_d^2 < 0, \quad \forall \psi_d \neq 0. \quad (12)$$

This proves that the desired heading angle asymptotically converges to 0, guiding the UAV on the line-of-sight to avoid the collision.

Theorem 2. For the ground speed of the ownship UAV less than that of the intruder UAV, i.e. $V < V_{in}$, the proposed collision avoidance guarantees the minimum separation if:

$$|\phi_{in} - \phi - \psi_d| \leq \sin^{-1} \frac{V}{V_{in}} \quad (13)$$

Proof. From geometric relationship in Fig. 4, the collision avoidance trajectory of the UAV with respect to a moving intruder satisfies that:

$$\frac{s}{t_c} = V_{in} \cos(\phi_{in} - \phi - \psi_d) - \sqrt{V^2 - V_{in}^2 \sin^2(\phi_{in} - \phi - \psi_d)}, \quad (14)$$

where s is the length of the tangent line to avoid the collision, and t_c is the time that the UAV reaches the point of tangency. If $V^2 - V_{in}^2 \sin^2(\phi_{in} - \phi - \psi_d) \geq 0$, there exists a feasible trajectory s , and hence be able to avoid the intruder. For the details of the proof, refer to Shin et al. (2008).

Theorem 3. For $V \geq V_{in}$ and the maximum heading angle rate limited by r_{max} , the minimum separation is guaranteed if:

$$R_d \geq V_d \frac{\psi_d}{r_{max}} + R_0, \quad (15)$$

where V_d and R_d are relative velocity and range of the obstacle/intruder at the line-of-sight of ψ_d , respectively.

Proof. The minimum time required for completing the avoiding turn is

$$t_c \geq \frac{\psi_d}{r_{max}}. \quad (16)$$

In order to complete the turn before colliding, the distance of the UAV and obstacle/intruder should satisfy:

$$R_d - R_0 \geq V_d t_c \geq V_d \frac{\psi_d}{r_{max}}. \quad (17)$$

4. NUMERICAL SIMULATIONS

4.1 Simulation Setup

Numerical simulations are conducted to validate the performance of the proposed collision avoidance algorithm. Three obstacles are modelled from the no-fly-zones and buildings near the test site, Missolonghi Airport in Greece, but the distance between the obstacles is adjusted to create more challenging and dense environment. The velocity of both the ownship (V) and the intruder (V_{in}) is 14 m/s, and the minimum separation R_0 is 50 m. A hundred different scenarios are created near the obstacles, with different start and end points for both the UAV and the intruder. The trajectories of the intruder are derived from the proposed collision avoidance algorithm based on the differential geometry concept (DGC). For the DGC, the control gain K is set as 0.1. The recognition range $R_{i,RC}$ is set as three times of the obstacle radius for the polygonal obstacles, and R_{RC} as 250 m for the moving intruder.

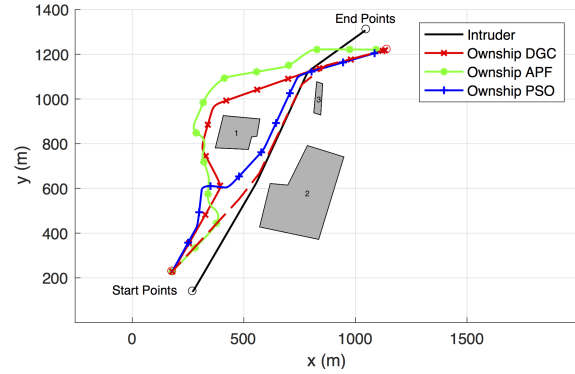


Fig. 5. Trajectory of Collision Avoidance Algorithms (Single Scenario)

To better assess the safety and efficiency of the proposed collision avoidance algorithm, two commonly used collision avoidance algorithms are used for comparison: artificial potential field method (APF), and particle swarm optimization method (PSO).

APF is designed to change the heading angle as Fajen et al. (2003):

$$\dot{\phi} = k_{way} \psi_{way} \left(e^{-\frac{R_{way}}{R_0}} + 1 \right) - k_{in} \psi_{in} e^{-\frac{R_{in}}{R_0}} - \sum_i k_{obs} \psi_{i,centre} e^{-\frac{R_{i,centre} - r_i}{R_0}}, \quad (18)$$

where r_i is the radius of the i -th obstacle, and the gain k_{way} is set as constant 0.1. The gains k_{in} and k_{obs} are set as 0.1 when the distance is within the range of 55 m and 75 m, respectively; otherwise, they are 0. Note that APF used in this paper changes only the heading angle in order to align with the assumptions used in the proposed algorithm. Also, the obstacles are considered as circular.

PSO is formulated to optimise the position of six intermediate waypoints to create a trajectory $(x(t), y(t))$ that avoids the obstacles while minimising the total flight time as:

$$\begin{aligned} \min J(x, y) &= t_f + \lambda f(x, y) + \lambda \sum_i g_i(x, y) \\ f(x, y) &= -\min \left(1 - \frac{R_{way}(t_f)}{10}, 0 \right) \\ g_i(x, y) &= \int_0^{t_f} \max \left(1 - \frac{R_i(t)}{R_0}, 0 \right) dt \end{aligned} \quad (19)$$

where t_f is the time of arrival at the end point, $f(x, y)$ is a constraint to arrive at the end point, $g_i(x, y)$'s are constraints to avoid the obstacle/intruder, and λ is a Lagrangian multiplier to impose the soft constraints, which is set as 100. For PSO algorithm, the number of particles are set as 150, and the maximum number of iteration is 50. Since PSO may converge to local minima depending on the initial condition, the most optimal scenario is chosen among 6 different random initiations. For the other parameter settings refer to Mostapha Kalami Heris (2015).

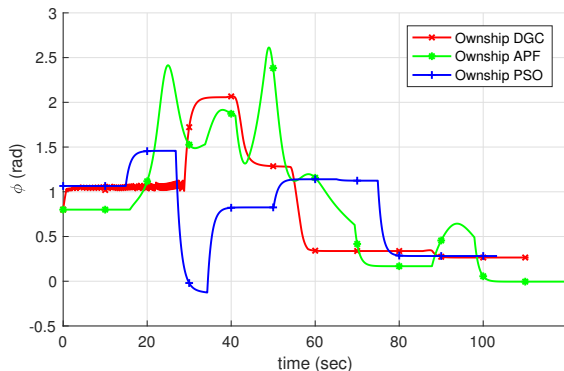


Fig. 6. Flight Angle of Collision Avoidance Algorithms (Single Scenario)

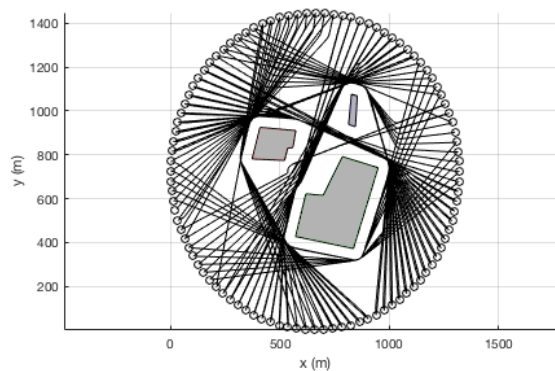


Fig. 8. Trajectories of the Intruder (100 Scenarios)

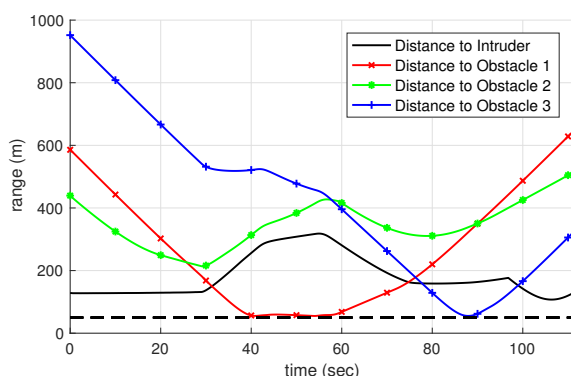


Fig. 7. Distance to Obstacles and Intruder Using the Proposed Collision Avoidance Algorithm (Single Scenario)

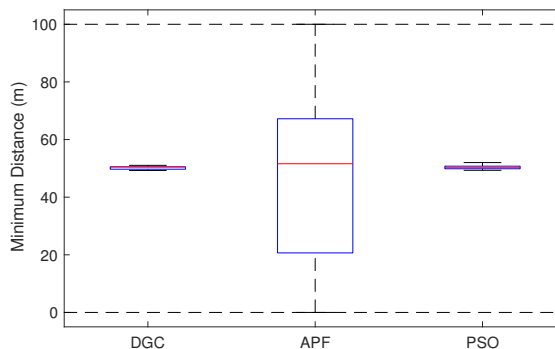


Fig. 9. Minimum Distance to Obstacles and Intruder of Collision Avoidance Algorithms (100 Scenarios)

4.2 Simulation Results

For a single scenario, the trajectories of different collision avoidance algorithms and their heading angle profiles are shown in Fig. 5 and Fig. 6. The intruder vehicle implemented with DGC goes through the obstacles to reach the end point. The trajectory of the ownship UAV without considering the intruder, shown in dashed line, also goes through the obstacles, resulting in the collision with the intruder. The ownship with DGC considering the intruder instead detours the obstacles to avoid the collision with the intruder. The distance of the ownship with DGC is shown in Fig. 7, validating that the minimum separation is guaranteed to all obstacles and intruder. The ownship with APF also detours the obstacles to avoid the collision, but the total flight time is longer since the obstacles are considered as circular shape and their repulsive effects are summed in APF. The ownship with PSO, which knows the trajectory of the intruder in advance, shows a slight detour in the first part but returns to go through the obstacles, resulting in the minimum flight time while avoiding the intruder. Considering that DGC and APF can be applied real-time unlike PSO, it is inferred that the proposed algorithm, DGC, can efficiently reach the target point with reasonable flight time, while maintaining the safety to guarantee the minimum separation.

For rigorous validation, the numerical simulations are conducted with 100 different scenarios, where the trajectories

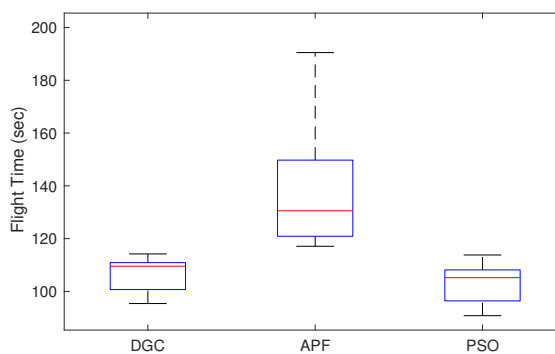


Fig. 10. Total Flight Time of Collision Avoidance Algorithms (100 Scenarios)

for the intruder with DGC are visualised in Fig. 8. For each algorithm for 100 scenarios, two performance metrics, minimum distance to obstacles/intruder and total flight time to reach the target point, are shown in Fig. 9 and Fig. 10. In Fig. 9, it is shown that DGC and PSO strictly guarantees the minimum separation, 50 m, in almost all scenarios, whereas the minimum distance of APF shows large variance and sometimes not guaranteed. Note that the negative distance means that the UAV is inside the polygonal obstacle. It shows that APF suffers from a widely know issue – narrow channel problem – in challenging environments. In Fig. 10, PSO shows the best efficiency in average, and DGC follows with smaller

variance. The flight time of APF is much longer than the other algorithms for larger detour, as inferred from Fig. 9. Another important performance metric to be compared is the computational cost, and the average computational time for each scenario has been 0.2 sec, 0.1 sec, and 163 sec for DGC, APF, and PSO, respectively. Comparing the three performance metrics – minimum distance, flight time, and computational cost – the proposed algorithm DGC guarantees the safety with reasonable efficiency and computational cost.

5. CONCLUSION

In this paper, a collision avoidance algorithm based on differential geometry concept has been proposed to consider multiple irregularly shaped no-fly-zones and other obstacles. The proposed algorithm has been addressed in two steps, conflict detection and resolution, and has been analytically proven that the minimum separation is guaranteed. The numerical simulations have verified not only that the minimum separation is guaranteed, but that the total flight time is close to optimal with low computational cost. This suggests that the proposed collision avoidance algorithm can be a practical and efficient solution for UTM, which requires safety and scalability.

ACKNOWLEDGEMENTS

The authors gratefully acknowledge that this research was supported by EuroDRONE project (No. SJU/LC/0342-CRT) under European Union's Horizon 2020 research and innovation programme.

REFERENCES

- Fajen, B.R., Warren, W.H., Temizer, S., and Kaelbling, L.P. (2003). A dynamical model of visually-guided steering, obstacle avoidance, and route selection. *International Journal of Computer Vision*, 54(1-3), 13–34.
- Hwang, I., Kim, J., and Tomlin, C. (2007). Protocol-based conflict resolution for air traffic control. *Air Traffic Control Quarterly*, 15(1), 1–34.
- Hwang, I. and Tomlin, C. (2002). Protocol-based conflict resolution for finite information horizon. In *Proceedings of the 2002 American Control Conference (IEEE Cat. No. CH37301)*, volume 1, 748–753. IEEE.
- Kelly III, W. and Eby, M. (2000). Advances in force field conflict resolution algorithms. In *AIAA guidance, navigation, and control conference and exhibit*, 4360.
- Mostapha Kalami Heris, S. (2015). Path planning using pso in matlab. *Khaje Nasir Toosi University of Technology*.
- Nieuwenhuisen, M., Schadler, M., and Behnke, S. (2013). Predictive potential field-based collision avoidance for multicopters. *Int. Arch. Photogramm. Remote Sens. Spatial Inf. Sci.*, 1, W2.
- Richards, A. and How, J.P. (2002). Aircraft trajectory planning with collision avoidance using mixed integer linear programming. In *Proceedings of the 2002 American Control Conference (IEEE Cat. No. CH37301)*, volume 3, 1936–1941. IEEE.
- Roberge, V., Tarbouchi, M., and Labonté, G. (2012). Comparison of parallel genetic algorithm and particle swarm optimization for real-time uav path planning. *IEEE Transactions on Industrial Informatics*, 9(1), 132–141.
- Seo, J., Kim, Y., and Tsourdos, A. (2013). Differential geometry based collision avoidance guidance for multiple uavs. *IFAC Proceedings Volumes*, 46(19), 113–118.
- Shin, H.S., Tsourdos, A., White, B., Shanmugavel, M., and Tahk, M.J. (2008). Uav conflict detection and resolution for static and dynamic obstacles. In *AIAA Guidance, Navigation and Control Conference and Exhibit*, 6521.
- Sun, J., Tang, J., and Lao, S. (2017). Collision avoidance for cooperative uavs with optimized artificial potential field algorithm. *IEEE Access*, 5, 18382–18390.
- White, B.A., Shin, H.S., and Tsourdos, A. (2011). Uav obstacle avoidance using differential geometry concepts. *IFAC Proceedings Volumes*, 44(1), 6325–6330.
- Yan, Z., Li, J., Zhang, G., and Wu, Y. (2018). A real-time reaction obstacle avoidance algorithm for autonomous underwater vehicles in unknown environments. *Sensors*, 18(2), 438.
- Yang, L., Zhang, X., Zhang, Y., and Xiangmin, G. (2019). Collision free 4d path planning for multiple uavs based on spatial refined voting mechanism and pso approach. *Chinese Journal of Aeronautics*.